

# Multiple actions of U-37883A, an ATP-sensitive $K^+$ channel blocker, on membrane currents in pig urethra

Toshihisa Tomoda <sup>a,b</sup>, Takakazu Yunoki <sup>b</sup>, Seiji Naito <sup>b</sup>, Yushi Ito <sup>a</sup>, Noriyoshi Teramoto <sup>a,\*</sup>

<sup>a</sup> Department of Pharmacology, Graduate School of Medical Sciences, Kyushu University, Fukuoka, 812-8582, Japan

<sup>b</sup> Department of Urology, Graduate School of Medical Sciences, Kyushu University, 3-1-1 Maidashi, Higashi Ward, Fukuoka, 812-8582, Japan

Received 4 April 2005; received in revised form 8 August 2005; accepted 18 August 2005

Available online 19 October 2005

## Abstract

The effects of U-37883A, a vascular ATP-sensitive  $K^+$  channel ( $K_{ATP}$  channel) blocker, on membrane currents were investigated in pig urethral myocytes by use of patch-clamp techniques (conventional whole-cell recordings, nystatin-perforated patches and cell-attached configuration). Tension measurement was also performed to study the effects of U-37883A on the levromakalim-induced urethral relaxation and the urethral resting tone in the absence and presence of Bay K 8644. Although cumulative application of U-37883A produced a concentration-dependent inhibitory effect on the levromakalim-induced urethral relaxation, U-37883A did not abolish the relaxation. In nystatin-perforated patch recording,  $K_{ATP}$  currents activated by levromakalim were inhibited by U-37883A in a concentration-dependent manner ( $K_i$ , 4.7  $\mu$ M). Approximately 10% of the  $K_{ATP}$  currents still remained even in the presence of 300  $\mu$ M U-37883A. In cell-attached mode, extracellular application of U-37883A (100  $\mu$ M) irreversibly inhibited the activity of the levromakalim-induced  $K_{ATP}$  channels. In whole-cell configuration, U-37883A suppressed the peak amplitude of voltage-dependent  $Ba^{2+}$  currents in a concentration- and voltage-dependent manner, and at 30  $\mu$ M, shifted the steady-state inactivation curve of the  $Ba^{2+}$  currents to the left at  $-90$  mV. These results demonstrate that U-37883A reduces not only the activities of  $K_{ATP}$  channels but also voltage-dependent  $Ca^{2+}$  channels. Therefore, it is not appropriate to define U-37883A as solely a vascular  $K_{ATP}$  channel blocker.

© 2005 Elsevier B.V. All rights reserved.

**Keywords:** ATP-sensitive  $K^+$  channels; Channel pore; U-37883A; Voltage-dependent  $Ca^{2+}$  channels

## 1. Introduction

Recent molecular studies have revealed that ATP-sensitive  $K^+$  channels ( $K_{ATP}$  channels) are an octomeric complex of four sulphonylurea receptors (SURs) and four pore-forming subunits of the inwardly rectifying  $K^+$  channel Kir6.x (Aguilar-Bryan et al., 1995; Inagaki et al., 1995). In functional expression studies, it is generally believed that SUR1/Kir6.2 represents the pancreatic  $\beta$ -cell  $K_{ATP}$  channel, that SUR2A/Kir6.2 represents the cardiac  $K_{ATP}$  channel, whereas SUR2B/Kir6.1 may represent the vascular smooth muscle-type of  $K_{ATP}$  channel (Babenko et al., 1998).

U-37883A (PNU-37883A, 4-morpholinecarboximidine-*N*-1-adamantyl-*N'*-cyclohexyl hydrochloride) has been developed as a non-sulphonylurea drug which has inhibitory actions on

vascular  $K_{ATP}$  channels at submicromolar concentrations. Since high concentrations of U-37883A ( $\geq 10$   $\mu$ M) showed no inhibitory effect on the activity of pancreatic, cardiac and skeletal  $K_{ATP}$  channels (Meisheri et al., 1993; Wellman et al., 1999), U-37883A has generally been thought to be a selective inhibitor of vascular  $K_{ATP}$  channels, which contain Kir6.1 subunits in the pore region.

However, it has been reported that U-37883A also suppress various other types of  $K^+$  channels (low conductance apical  $K^+$  channels in thick ascending limb of the loop of Henle, Wang et al., 1995; dopamine-modulated  $K^+$  channels, Lin et al., 1998; Shaker  $K^+$  currents, Surah-Narwal et al., 1999; intracellular  $Ca^{2+}$ -activated large conductance  $K^+$  channels i.e.  $BK_{Ca}$  channels, Teramoto et al., 2004), suggesting that U-37883A is unlikely to be a selective blocker for vascular  $K_{ATP}$  channels. Despite its frequent use as a pharmacological tool, even in freshly dispersed smooth muscle cells,  $K^+$  channels targeted by U-37883A remain to be identified by use of single-channel

\* Corresponding author. Tel.: +81 92 642 6077; fax: +81 92 642 6079.

E-mail address: [noritera@med.kyushu-u.ac.jp](mailto:noritera@med.kyushu-u.ac.jp) (N. Teramoto).

recordings. In this report, using single-channel recordings, we have investigated the effects of U-37883A on glibenclamide-sensitive  $K^+$  channels (i.e.  $K_{ATP}$  channels) in pig urethral myocytes in order to compare the potency of U-37883A and the specificity of U-37883A with voltage-dependent  $Ba^{2+}$  inward currents through voltage-dependent L-type  $Ca^{2+}$  channels.

## 2. Material and methods

### 2.1. Tension measurement

Fresh urethra from female pigs were collected from a local abattoir. For tension measurement, modified Krebs solution was used (mM):  $Na^+$  137,  $K^+$  5.9,  $Mg^{2+}$  1.2,  $Ca^{2+}$  2.5,  $Cl^-$  133.7,  $HCO_3^-$  15.4,  $H_2PO_4^-$  1.2 and glucose 11.5 which was bubbled with 97%  $O_2$  and 3%  $CO_2$ . Fine strips were prepared as described previously (Teramoto and Ito, 1999). An initial tension equivalent to 1 g weight was applied to each strip. Strips were then allowed to equilibrate for approximately 1.5–2 h while the basal urethral tone developed and became stable (37 °C). To prevent both noradrenaline outflow from sympathetic nerve terminals and  $\beta$ -adrenoceptor stimulation, 3  $\mu$ M guanethidine and 0.3  $\mu$ M propranolol were present throughout the experiments. Data were recorded on a Macintosh G4 computer, through “MacLab 3.5.6” (ADInstruments Pty Ltd., Castle Hill, Australia). The tension was expressed as g/mg of tissue.

### 2.2. Cell dispersion and recording procedure of patch-clamp experiments

Pig urethral smooth muscle strips were treated with papain and collagenase in  $Ca^{2+}$ -free solution and myocytes were freshly isolated by the gentle tapping method (Teramoto and Brading, 1996). Relaxed spindle-shaped cells were isolated and stored at 4 °C. The dispersed cells were normally used within 4 h for experiments. Patch-clamp experiments were performed at room temperature (21–23 °C) as described previously (Teramoto et al., 2003; 2004). The resistance of the patch pipette used was in the region of either 2–3 M $\Omega$  (macroscopic recordings) or 3–5 M $\Omega$  (single-channel recordings). Junction potentials between bath and pipette solutions were measured with a 3 M KCl reference electrode and were <2 mV, so that correction for these potentials was not made. Capacitance noise was kept to a minimum by maintaining the test solution in the electrode as low as possible. At the beginning of each experiment, the series resistance was compensated.

### 2.3. Drugs and solutions

For whole-cell recordings, the ionic composition of the physiological salt solution (PSS) in the bath was (mM):  $Na^+$  140,  $K^+$  5,  $Mg^{2+}$  1.2,  $Ca^{2+}$  2,  $Cl^-$  151.4, glucose 10, HEPES 10, and was titrated to pH 7.35–7.40 with Tris base. High  $K^+$  pipette solution contained (mM):  $K^+$  140,  $Cl^-$  140, glucose 5, EGTA 5, and HEPES 10/Tris (pH 7.35–7.40). The perforated-patch technique with nystatin was also occasionally used to

record whole-cell currents (Teramoto and Brading, 1996). In short, nystatin was freshly dissolved in acidified methanol (1 N HCl to about pH 2) and the pH was adjusted to 7.4 with Tris base. This stock solution (10 mg/ml) was diluted in the pipette solution at a final concentration of 50  $\mu$ g/ml just before use. Whole-cell recording was performed with a pipette which was first dipped in normal pipette solution (nystatin-free) and then back-filled with nystatin-containing pipette solution. This resulted in chemical perforation of the membrane. The following solutions were used: 140 mM  $K^+$  solution containing (mM):  $Na^+$  5,  $K^+$  140,  $Mg^{2+}$  1.2,  $Ca^{2+}$  2, glucose 5,  $Cl^-$  151.4, HEPES 10, titrated to pH 7.35–7.40 with Tris base; high potassium pipette solution containing (mM):  $K^+$  140,  $Cl^-$  140, glucose 5, EGTA 5, and HEPES 10/Tris (pH 7.35–7.40). For cell-attached recordings, the pipette and bath solution were high potassium solutions (mM):  $K^+$  140,  $Cl^-$  140, EGTA 5, glucose 5, HEPES 10/Tris (pH 7.35–7.40). For recording voltage-dependent  $Ba^{2+}$  currents in whole-cell configuration, high caesium pipette solution contained (mM):  $Cs^+$  130, tetraethylammonium ( $TEA^+$ ) 10,  $Mg^{2+}$  2,  $Cl^-$  144, glucose 5, EGTA 5, ATP 5, HEPES 10/Tris (pH 7.35–7.40).  $Ba^{2+}$  10 mM bath solution contained (mM):  $Ba^{2+}$  10,  $TEA^+$  135,  $Cl^-$  155, glucose 10, HEPES 10/Tris (pH 7.35–7.40). Cells were allowed to settle in the small experimental chamber (80  $\mu$ l in volume). The bath solution was superfused by gravity throughout the experiments at a rate of 2 ml/min. U-37883A was purchased from BIOMOL Research Laboratories Inc. (PA, U.S.A.). Levromakalim (kindly provided by SmithKline Beecham, U.K.) and Bay K 8644 were prepared daily as a 100 mM stock solution in dimethyl sulphoxide (DMSO). The final concentration of DMSO was less than 0.3% and this concentration did not affect either the membrane currents or the potassium channels. All other rest drugs were obtained from Sigma Chemical (Sigma Chemical K.K., Tokyo, Japan).

### 2.4. Data analysis and statistics

For single-channel recordings, the stored data were low-pass filtered at 2 kHz (–3 dB) and sampled into the computer with a digitalized interval of 80  $\mu$ s. No correction was made for missing events (events briefer than 80  $\mu$ s). In Fig. 4A, continuous traces in the figures were obtained from records filtered at 500 Hz for presentation (digital sampling interval, 25 ms). Values for the channel open state probability ( $P_{open}$ ) were measured for 1 or 2 min,

$$NP_o = \left( \sum_{j=1}^N t_j \cdot j \right) / T$$

where  $t_j$  is the time spent at each current level corresponding to  $j=0, 1, 2, \dots, N$ ,  $T$  is the duration of the recording, and  $N$  is taken as the maximum number of channels observed in the patch membrane where  $P_{open}$  was relatively high. Data points were fitted using a least-squares fitting.

The dissociation constant for drug binding to the channel in the inactivated state can be estimated from the shift of the

voltage-dependent inactivation curve and the concentration response curve obtained at the resting state by use of the following equation (Uehara and Hume, 1985),

$$-\Delta V_{\text{half}} = k \cdot \ln\{(1 + [D]/K_{\text{inact}})/(1 + [D]/K_{\text{rest}})\}$$

where  $\Delta V_{\text{half}}$  is the amplitude of the shift of the voltage-dependent inactivation curve,  $k$  is a slope factor for the inactivation curve and  $[D]$  is the concentration of drug applied.  $K_{\text{inact}}$  and  $K_{\text{rest}}$  are dissociation constants of U-37883A for the inactivated and the resting states of voltage-dependent  $\text{Ca}^{2+}$  channels, respectively.

Statistical analyses were performed with analysis of variance (ANOVA) test (two-factor with replication). Changes were considered significant at  $P < 0.01$ . Data are expressed as mean with the standard deviation (S.D.).

### 3. Results

#### 3.1. Comparison between SNP- and levromakalim-induced relaxations in pig urethra

In order to investigate the effects of U-37883A on the levromakalim-induced urethral relaxation, urethral relaxing mechanisms were compared between sodium nitroprusside (SNP), an exogenous nitric oxide generator, and levroma-

kalim, an ATP-sensitive  $\text{K}^+$  channel ( $\text{K}_{\text{ATP}}$  channel) opener. Fig. 1A shows that application of SNP caused urethral relaxation that was maximal at 10  $\mu\text{M}$ . After recovery, a supramaximal concentration of levromakalim (10  $\mu\text{M}$ ) caused a relaxation of the same relative amplitude (SNP,  $1.01 \pm 0.01$ ,  $n=6$ ) when the peak amplitude of the levromakalim-induced relaxation was normalized as one. However, the time taken to reach peak relaxation was noticeably quicker with 10  $\mu\text{M}$  SNP (SNP,  $1.1 \pm 0.2$  min, vs. levromakalim,  $2.5 \pm 0.6$  min,  $n=6$ ; Fig. 1B). Subsequent application of glibenclamide (1–10  $\mu\text{M}$ ) had no effect on the 10  $\mu\text{M}$  SNP-induced relaxation ( $n=6$ , Fig. 1C).

#### 3.2. Effects of U-37883A on the levromakalim-induced relaxation

As shown in Fig. 1D, levromakalim (1  $\mu\text{M}$ ) produced a slow relaxation which reached a level similar to the maximum relaxation produced by 10  $\mu\text{M}$  levromakalim (Teramoto and Ito, 1999). Cumulative application of U-37883A produced a concentration-dependent inhibition of the 1  $\mu\text{M}$  levromakalim-induced urethral relaxation with a  $K_i$  of 0.7  $\mu\text{M}$  (Fig. 1F). However, U-37883A did not abolish the relaxation and a small U-37883A-insensitive component remained (3  $\mu\text{M}$ ,  $0.21 \pm 0.17$ ,  $n=5$ ; 10  $\mu\text{M}$ ,  $0.16 \pm 0.13$ ,  $n=5$ , maximum value of the relaxation normalized as one) as shown in Fig. 1D

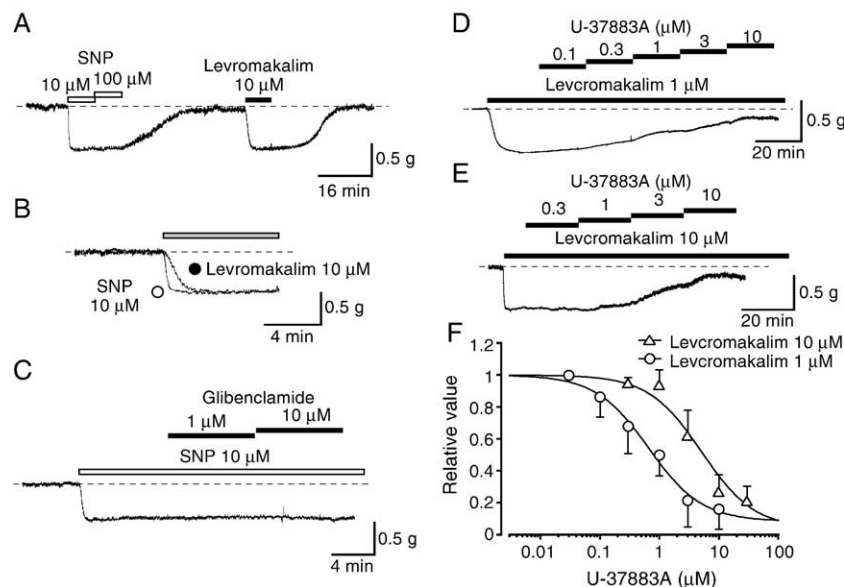


Fig. 1. The sodium nitroprusside (SNP)- and the levromakalim-induced relaxations in pig proximal urethra. The dashed line indicates the mean resting urethral tone. (A) The effects of SNP (10 and 100  $\mu\text{M}$ ) and 10  $\mu\text{M}$  levromakalim on the resting urethral tone. (B) Superimposition of the 10  $\mu\text{M}$  SNP (open circle) and the 10  $\mu\text{M}$  levromakalim-induced relaxation (filled circle). The hatched bar indicates the application of both drugs (8 min duration). (C) Additional application of glibenclamide (1 and 10  $\mu\text{M}$ ) had no effect on the 10  $\mu\text{M}$  SNP-induced urethral relaxation. (D) The effects of cumulative addition of U-37883A (0.1–10  $\mu\text{M}$ ) on the 1  $\mu\text{M}$  levromakalim-induced relaxation. (E) The effects of cumulative addition of U-37883A (0.3–10  $\mu\text{M}$ ) on the 10  $\mu\text{M}$  levromakalim-induced relaxation. (F) Relationships between the relative inhibitory value of levromakalim-induced urethral relaxation and the concentration of U-37883A. The peak amplitude of the levromakalim-induced relaxation was normalized as one.

$$\text{Relative amplitude} = C + (1-C)[1/\{1 + (K_i/D)^{n_H}\}]$$

where  $K_i$ ,  $C$ ,  $D$  and  $n_H$  are the inhibitory dissociation constant, the value of the U-37883A-insensitive component, concentration of U-37883A ( $\mu\text{M}$ ) and Hill's coefficient, respectively. The following values were calculated for the curve fitting by use of the least-squares method:  $K_i=0.7$   $\mu\text{M}$ ,  $n_H=1$ ,  $C=0.08$  (1  $\mu\text{M}$  levromakalim,  $n=3-8$ );  $K_i=5.1$   $\mu\text{M}$ ,  $n_H=1$ ,  $C=0.03$  (10  $\mu\text{M}$  levromakalim,  $n=5-10$ ). Each symbol indicates mean with S.D. shown by vertical lines. Some of the

and F. Similarly, U-37883A (0.3–10  $\mu\text{M}$ ) reduced the 10  $\mu\text{M}$  levcromakalim-induced relaxation in a cumulative manner ( $K_i$ , 5  $\mu\text{M}$ ), but did not abolish it (Fig. 1E, F).

### 3.3. Inhibitory effects of U-37883A on the levcromakalim-induced glibenclamide-sensitive macroscopic and unitary $K_{\text{ATP}}$ currents

After the nystatin-perforated patch had been established, an inward current was evoked by application of levcromakalim (100  $\mu\text{M}$ ) in symmetrical 140 mM  $\text{K}^+$  conditions at  $-50$  mV (Fig. 2A). When U-37883A was applied in a cumulative manner (3–10  $\mu\text{M}$ ), it caused an inhibition of the basal amplitude of the levcromakalim-induced current. However, as shown in Fig. 2B, a small but significant U-37883A-insensitive levcromakalim-induced current ( $12 \pm 4\%$ ,  $n=5$ ), which was abolished by 100  $\mu\text{M}$  glibenclamide, was observed even in the presence of 300  $\mu\text{M}$  U-37883A. Fig. 2C shows concentration-dependent inhibitory effects of U-37883A on the levcromakalim-induced inward current at  $-50$  mV ( $K_i=4.7$   $\mu\text{M}$ ).

Further studies were carried out of the effects of 100  $\mu\text{M}$  U-37883A on the 100  $\mu\text{M}$  levcromakalim-induced inward  $\text{K}^+$  currents using triangular ramp potential pulses (see inset in Fig. 3A). Four of these were applied from  $-120$  mV to  $+20$  mV, obtaining the current–voltage relationships in the absence and presence of 100  $\mu\text{M}$  U-37883A. Fig. 3A shows the expected reduction of the levcromakalim-induced inward current on application of 100  $\mu\text{M}$  U-37883A. Note that approximate 10% ( $0.08 \pm 0.02$ ,  $n=4$ ) of the levcromakalim-induced current still remained even in the presence of 100  $\mu\text{M}$  U-37883A. Fig. 3B shows the averaged membrane currents during the falling phase of the ramp pulses under the various experimental conditions. The 100  $\mu\text{M}$  U-37883A-sensitive membrane current in the presence of levcromakalim was obtained by subtracting the mean membrane current in the presence of 100  $\mu\text{M}$  U-37883A from the membrane current in its absence.

To investigate further the U-37883A-sensitive  $\text{K}^+$  currents, single-channel recordings were performed at  $-50$  mV using the cell-attached mode (Fig. 4A). Fig. 4A shows the effects of U-37883A (10–100  $\mu\text{M}$ ) on the levcromakalim-induced  $\text{K}_{\text{ATP}}$  channels (pipette and bath solution, 140 mM  $\text{K}^+$  solution). When levcromakalim (100  $\mu\text{M}$ ) was applied, a unitary current ( $\text{K}_{\text{ATP}}$  channel; 2.1 pA, obtained from the all-points amplitude histogram) was evoked (Fig. 4B). The  $NP_{\text{open}}$  value of  $\text{K}_{\text{ATP}}$  channels for 2 min duration was calculated to be 1.51. Extracellular application of U-37883A ( $\leq 30$   $\mu\text{M}$ ) had little effect on the  $NP_{\text{open}}$  value (Fig. 4A, C). However, when 100  $\mu\text{M}$  U-37883A was applied to the bath, channel opening was inhibited (Fig. 4B,  $NP_{\text{open}}$  value, 0.38), without changing the unitary amplitude. On removal of U-37883A, channel opening gradually reappeared although the  $NP_{\text{open}}$  value did not recover to the control level (Fig. 4A, C). Subsequent application of 10  $\mu\text{M}$  glibenclamide suppressed the activity. Similar observations were obtained in three other patches. On the other hand, if 100  $\mu\text{M}$  U-37883A was included in the pipette solution with the

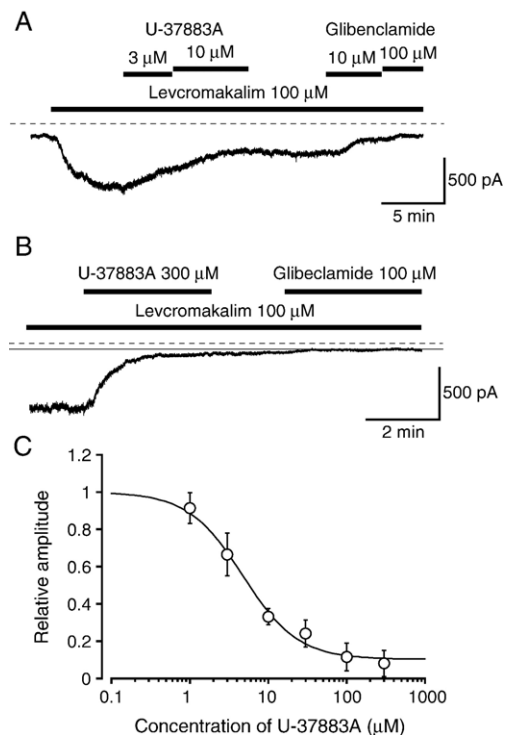


Fig. 2. Inhibitory effects of U-37883A on the levcromakalim-induced glibenclamide-sensitive inward  $\text{K}^+$  current recorded using a nystatin-perforated patch at a holding potential of  $-50$  mV (bath solution, 140 mM  $\text{K}^+$  solution; pipette solution, 140 mM  $\text{K}^+$  containing 5 mM EGTA). (A) Current trace. Levcromakalim (100  $\mu\text{M}$ ) caused an inward membrane current (peak amplitude approximately 500 pA). Currents were measured from the 100  $\mu\text{M}$  glibenclamide-sensitive current level. The current was inhibited by application of U-37883A in a concentration-dependent manner and was then suppressed by glibenclamide (10–100  $\mu\text{M}$ ). The dashed line indicates zero current line. (B) A small but detectable glibenclamide-sensitive inward current was observed even after application of 300  $\mu\text{M}$  U-37883A. The dashed line indicates zero current line and the full line indicates the 100  $\mu\text{M}$  glibenclamide-sensitive level. (C) Concentration–response curve of U-37883A. The peak amplitude of the 100  $\mu\text{M}$  levcromakalim-induced current (measured over the final 30 s before application of U-37883A) was taken as one, measured from the current level in the presence of 100  $\mu\text{M}$  glibenclamide. The curve was drawn by fitting the following equation using the least-squares method,

$$\text{Relative amplitude} = C + (1-C)[1/\{1 + (K_i/D)n_H\}]$$

where  $K_i$ ,  $C$ ,  $D$  and  $n_H$  are the inhibitory dissociation constant, the value of the U-37883A-insensitive component, concentration of U-37883A ( $\mu\text{M}$ ) and Hill's coefficient, respectively. The following values were used for the curve fitting:

cell-attached configuration, extracellular application of levcromakalim never appeared to activate  $\text{K}_{\text{ATP}}$  channels ( $n=26$ ).

### 3.4. Effects of U-37883A on the urethral tone in the absence and presence of Bay K 8644

Although U-37883A ( $\leq 1$   $\mu\text{M}$ ) possessed little effect on the resting tone of pig urethra, U-37883A ( $\geq 3$   $\mu\text{M}$ ) caused a significant relaxation (Fig. 5A, C). Bay K 8644, a selective voltage-dependent L-type  $\text{Ca}^{2+}$  channel agonist, caused a dramatic increase in the resting tone (Fig. 5B). In the presence of Bay K8644, U-37883A ( $\geq 3$   $\mu\text{M}$ ) also caused



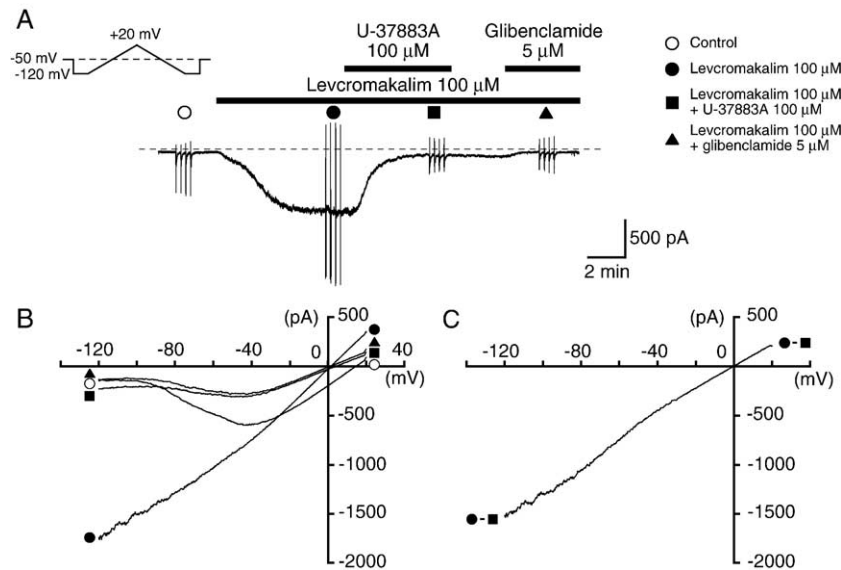


Fig. 3. Inhibitory effects of U-37883A on the levcromakalim-induced glibenclamide-sensitive inward  $K^+$  current at  $-50$  mV (bath solution, 140 mM  $K^+$  solution; pipette solution, 140 mM  $K^+$  containing 5 mM EGTA) in nystatin-perforated patch. (A) Current trace. The vertical lines are responses to triangular ramp potential pulses of  $200$  mV  $s^{-1}$  from  $-120$  to  $+20$  mV, applied after an initial 300 ms conditioning pulse to  $-120$  mV (see inset). Levcromakalim ( $100$   $\mu$ M) caused an inward membrane current (peak amplitude,  $845$  pA). The current was suppressed by application of  $100$   $\mu$ M U-37883A, recovered to a steady state amplitude after U-37883A was removed, and was then suppressed by  $5$   $\mu$ M glibenclamide. The dashed line indicates zero current line. (B) The current–voltage curves measured from the negative-going limb (the falling phase) of the ramp pulse. Each symbol is the same as in the current trace. The lines are mean membrane currents from the four ramps in each condition. (C) Net membrane currents. The U-37883A-sensitive membrane current was obtained from the membrane currents in the absence and presence of  $100$   $\mu$ M U-37883A when levcromakalim was present in the bath solution.

a concentration-dependent relaxation (Fig 5B, C). The U-37883A-induced relaxation was expressed as a relative value when the amplitude of the  $10$   $\mu$ M SNP was normalized as 1.0.

Note that the maximum level of relaxation achieved by  $10$   $\mu$ M SNP showed no significant difference in the presence and absence of  $1$   $\mu$ M Bay K 8644 (data not shown).

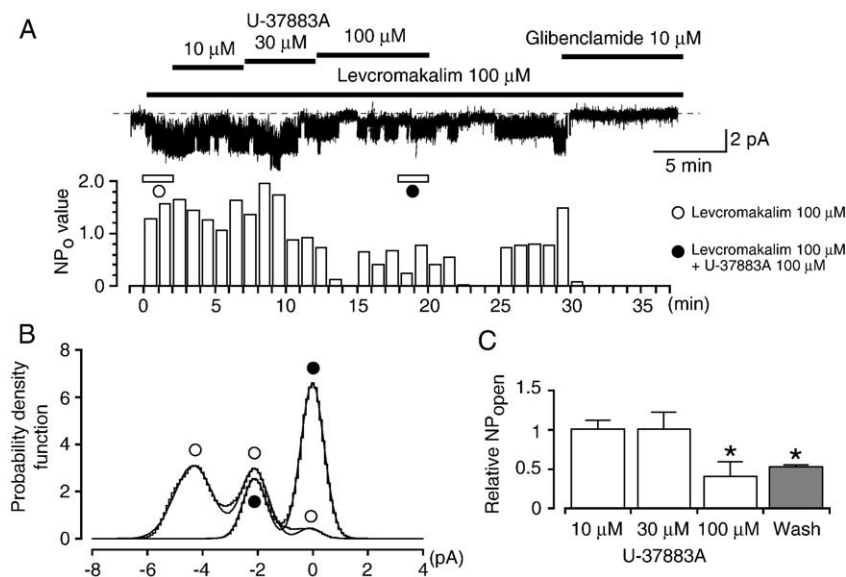


Fig. 4. Effects of U-37883A on the  $100$   $\mu$ M levcromakalim-induced  $K_{ATP}$  channels. Cell-attached patch at  $-50$  mV. Levcromakalim  $100$   $\mu$ M was added to the bath solution. (A) Current trace of the effects of each concentration of U-37883A on the activity of  $K_{ATP}$  channels, with the  $NP_{open}$  values shown below, calculated for every 1 min segment of the record (time 0 indicates the time when  $K_{ATP}$  channel activity was evoked by levcromakalim). Subsequently, application of  $10$   $\mu$ M glibenclamide suppressed the activity of the  $2.1$  pA  $K^+$  channel. The dashed line indicates the current when the channel was not open. (B) All-point amplitude histograms in the presence of  $100$   $\mu$ M U-37883A obtained during the last 2 min of a 6 min application. Histograms in the absence (control; just before the application of U-37883A for 2 min) or presence of U-37883A were superimposed. Continuous lines in the histograms are theoretical curves fitted with the Gaussian distribution, by the least-squares method. The abscissa scales show the amplitude of the current (pA) and the ordinate scales show the percentage value of the probability density function (%) for the recording period (2 min). Each symbol is the same as in (A). (C) The relative  $NP_{open}$  values ( $\pm$ S.D.) in the presence of U-37883A ( $10$ ,  $30$  and  $100$   $\mu$ M), after washing-out U-37883A and in the presence of  $10$   $\mu$ M glibenclamide, when the control value in each patch was normalized to one ( $n=4$ ). \*Significantly different from the control (ANOVA,  $P<0.01$ ).

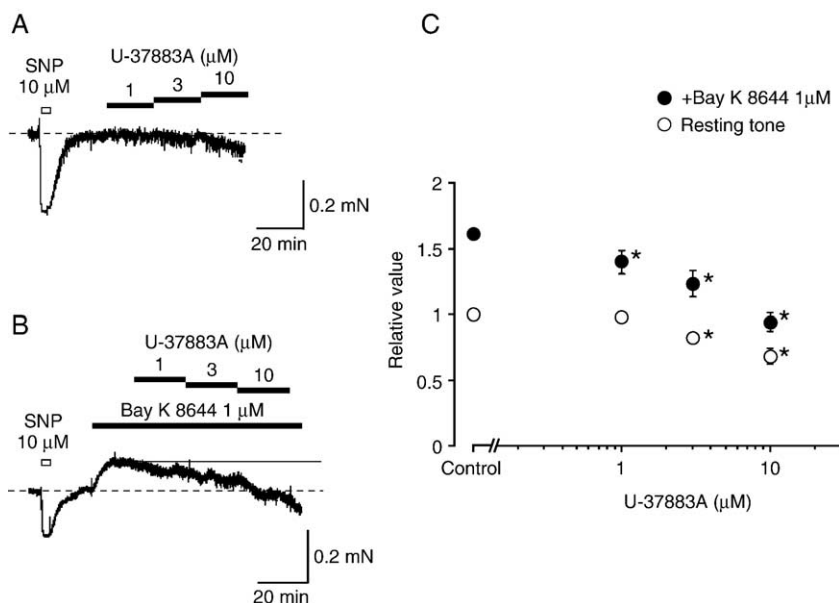


Fig. 5. The relaxing effects of U-37883A on the urethral tone in the absence and presence of Bay K8644. (A) The effects of U-37883A on the urethral tone. The dashed line indicates the mean resting urethral tone. (B) The effects of U-37883A on the urethral tone in the presence of 1 μM Bay K 8644. The line indicates the increased urethral tone in the presence of Bay K 8644. The dashed line indicates the mean resting urethral tone. (C) Relationships between the relative value of the U-37883A-induced relaxation and the concentration of U-37883A. The peak amplitude of the 10 μM SNP-induced relaxation was taken as one in the absence of Bay K 8644. Each symbol indicates mean with S.D. shown by vertical lines ( $n=4$ ). \*Significantly different from the relative value before application of U-37883A in each experimental condition ( $t$ -test,  $p<0.01$ ).

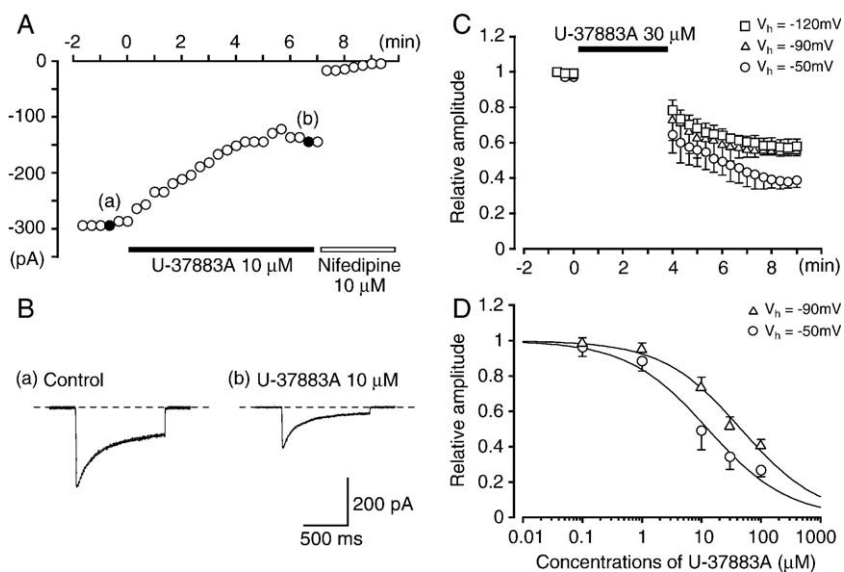


Fig. 6. The effect of U-37883A on voltage-dependent  $Ba^{2+}$  currents. Whole-cell recording, pipette solution  $Cs^+$ -TEA $^+$  solution containing 5 mM EGTA and the bath solution 10 mM  $Ba^{2+}$  containing 135 mM TEA $^+$ . (A) Effects of 10 μM U-37883A and 10 μM nifedipine on voltage-dependent  $Ba^{2+}$  currents in pig urethra. The time course of the effects of application of the two antagonists (U-37883A and nifedipine). Time 0 indicates the time when 10 μM U-37883A was applied to the bath. (B) Original current traces before (control, (A)) and after application of 10 μM U-37883A (B), as indicated in (A). (C) No pulses were applied for the initial four min, after application of 30 μM U-37883A. Each symbol shows the mean value of relative amplitude of the voltage-dependent  $Ba^{2+}$  current evoked by the depolarizing pulses after this four min, from the three holding potentials (−50 mV, −90 mV and −120 mV) when the peak amplitude of the voltage-dependent  $Ba^{2+}$  current just before application of U-37883A was normalized as one (control). (D) Relationships between relative inhibition of the peak amplitude of  $Ba^{2+}$  current and the concentration of U-37883A at two holding potentials (−50 mV and −90 mV). The curves were drawn by fitting the following equation using the least-squares method:

$$\text{Relative amplitude of voltage-dependent } Ba^{2+} \text{ current} = 1 / \{1 + (D/K_i)^{n_H}\}$$

where  $K_i$ ,  $D$  and  $n_H$  are the inhibitory dissociation constant, concentration of U-37883A (μM) and Hill's coefficient, respectively. The following values were used for the curve fitting: −50 mV,  $K_i=13$  μM,  $n_H=0.7$ ; −90 mV,  $K_i=46$  μM,  $n_H=0.7$ . Each symbol indicates the mean of 5–6 observations with  $\pm$ S.D. shown by vertical

### 3.5. Actions of U-37883A on voltage-dependent $Ba^{2+}$ currents in pig urethra

To investigate further the effects of U-37883A on voltage-dependent  $Ca^{2+}$  currents, the conventional whole-cell configuration was performed.  $Ba^{2+}$  (10 mM) was used as a charge carrier in bath solution in order to isolate voltage-dependent inward currents through  $Ca^{2+}$  channels by inhibiting other  $Ca^{2+}$ -activated mechanisms (such as  $Ca^{2+}$ -activated  $K^+$  currents and  $Ca^{2+}$ -activated  $Cl^-$  currents etc.) and the pipette was filled with a  $Cs^+$ -TEA $^+$  solution containing 5 mM EGTA. Fig. 6A shows the time course of the effects of U-37883A (10  $\mu$ M) on the  $Ba^{2+}$  inward current evoked by a depolarizing pulse to +10 mV from a holding potential of -50 mV. The depolarizing pulses were applied every 20 s. U-37883A reduced the peak amplitude of the  $Ba^{2+}$  inward currents ( $0.49 \pm 0.11$ ,  $n=6$ ). Subsequently, 10  $\mu$ M nifedipine completely suppressed the  $Ba^{2+}$  inward currents. As shown in Fig. 6C, when a depolarizing pulse (to +10 mV) was applied after an interval of 4 min in the presence of 30  $\mu$ M U-37883A, the peak amplitude of the

$Ba^{2+}$  inward current was smaller than that observed before application of U-37883A; however, it was consistently larger than that recorded at 4 min with repetitive application of the depolarizing pulses (single pulse,  $0.65 \pm 0.1$ ,  $n=4$  vs. repetitive pulse  $0.34 \pm 0.07$ ,  $n=4$ ). Similarly, reduction of the peak amplitude in the first depolarizing pulse after 4 min was observed at two different holding potentials (-90 mV,  $0.73 \pm 0.12$ ,  $n=4$ ; -120 mV,  $0.78 \pm 0.06$ ,  $n=4$ ). The amplitude of the voltage-dependent  $Ba^{2+}$  currents evoked by a depolarizing pulse to +10 mV was the same at holding potentials more negative than -80 mV, where the peak amplitude of voltage-dependent  $Ba^{2+}$  currents before application of U-37883A was taken as one (-90 mV,  $0.73 \pm 0.12$ ,  $n=4$ ; -120 mV,  $0.78 \pm 0.06$ ,  $n=4$ ). Fig. 6D shows the relationships between the relative peak amplitude of  $Ba^{2+}$  inward currents evoked by a depolarizing pulse to 10 mV applied every 20 s and concentrations of U-37883A from two different holding potentials (-50 mV and -90 mV). U-37883A inhibited the peak amplitude of the  $Ba^{2+}$  inward currents in a concentration-dependent manner (-50 mV,  $K_i=13$   $\mu$ M; -90 mV,  $K_i=46$   $\mu$ M).

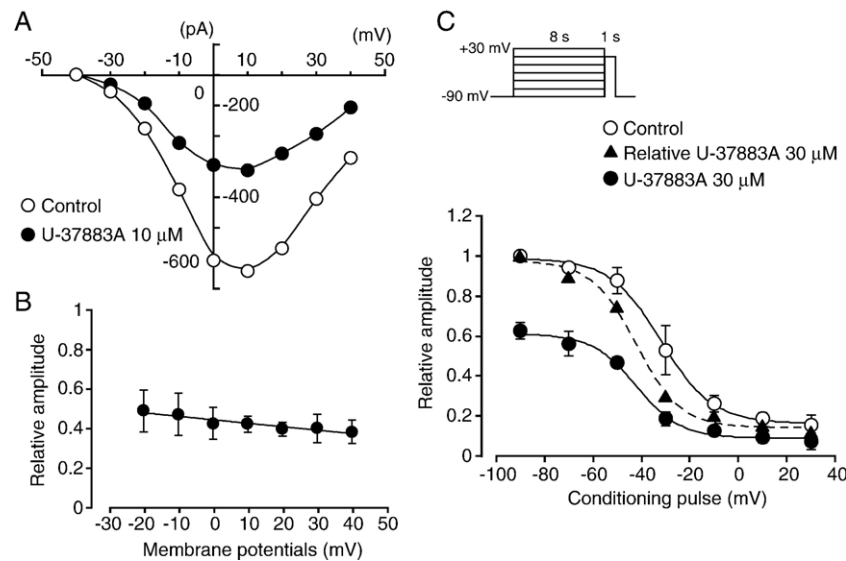


Fig. 7. Effects of U-37883A on voltage-dependent  $Ba^{2+}$  inward currents at a holding membrane potential of -50 mV in pig urethra. The pipette solution was  $Cs^+$ -TEA $^+$  solution containing 5 mM EGTA and the bath solution was 10 mM  $Ba^{2+}$  containing 135 mM TEA $^+$ . (A) Current-voltage relationships. The current amplitude was measured as the peak amplitude of the  $Ba^{2+}$  inward current in each condition. The lines were drawn by eye. (B) Relationship between the test potential and relative value of the  $Ba^{2+}$  inward currents inhibited by 10  $\mu$ M U-37883A, expressed as a fraction of the peak amplitude of the  $Ba^{2+}$  inward current evoked by various amplitudes of the depolarizing pulse in the absence of U-37883A. Each symbol indicates the mean of 4 observations with  $\pm$ S.D. shown by vertical lines. The line was drawn by eye. (C) Effects of U-37883A (30  $\mu$ M) on the voltage-dependent inactivation of the  $Ba^{2+}$  inward current in pig urethra at -90 mV. Whole-cell recording, pipette solution  $Cs^+$ -TEA $^+$  solution containing 5 mM EGTA and the bath solution 10 mM  $Ba^{2+}$  containing 135 mM TEA $^+$ . Conditioning pulses of various amplitudes were applied (up to +30 mV, 8 s duration) before application of the test pulse (to +10 mV, 1 s duration). An interval of 20 ms was allowed between these two pulses to estimate possible contamination of the capacitive current. The peak amplitude of the  $Ba^{2+}$  current evoked by each test pulse was measured before and after application of 30  $\mu$ M U-37883A. The curves with the solid line represent the peak amplitude of the  $Ba^{2+}$  inward current in the absence and presence of U-37883A without application of any conditioning pulse was normalized as one. The curve with the broken line was normalised to the current at +10 mV upon stepping from -90 mV in 30  $\mu$ M U-37883A. The lines were drawn by fitting the data to the following equation in the least-squares method,

$$I = (I_{\max} - C) / \{1 + \exp[(V - V_{\text{half}})/k]\} + C$$

where  $I$ ,  $I_{\max}$ ,  $V$ ,  $V_{\text{half}}$ ,  $k$  and  $C$  are the relative amplitude of  $Ba^{2+}$  inward currents observed at various amplitude of the conditioning pulse ( $I$ ) and observed with application of the conditioning pulse of -90 mV ( $I_{\max}$ ), amplitude of the conditioning pulse ( $V$ ), and that where the amplitude of  $Ba^{2+}$  inward current was reduced to half ( $V_{\text{half}}$ ), slope factor ( $k$ ) and fraction of the non-inactivating component of  $Ba^{2+}$  inward current ( $C$ ). The curves in the absence or presence of U-37883A were drawn using the following values: (control),  $I_{\max}=0.99$ ,  $V_{\text{half}}=-32$ ,  $k=10$  and  $C=0.16$ ; (U-37883A, 30  $\mu$ M),  $I_{\max}=0.97$ ,  $V_{\text{half}}=-42$ ,  $k=9.2$  and  $C=0.14$ . Each

### 3.6. Voltage-dependent inhibitory effects of U-37883A on voltage-dependent $Ba^{2+}$ currents

Fig. 7A shows the current-voltage relationships in the absence and presence of 10  $\mu$ M U-37883A. U-37883A inhibited the peak amplitude of the  $Ba^{2+}$  currents evoked by depolarizing pulses (1 s duration) from a holding potential of  $-50$  mV at levels more positive than  $-30$  mV, and the inhibition showed some voltage-dependency (Fig. 7B). This voltage-dependency was investigated before and after application of 30  $\mu$ M U-37883A using the experimental protocol shown in Fig. 7C (conditioning pulse duration, 8 s; holding membrane potential,  $-90$  mV). In the absence of U-37883A (control), inactivation of the  $Ba^{2+}$  current occurred with depolarizing pulses positive to  $-50$  mV. After application of 30  $\mu$ M U-37883A (approximately 5 min later), the voltage-dependent inactivation curve in the same cells was shifted to the left (Fig. 7C).

## 4. Discussion

The present study provides the first direct electrophysiological evidence for the actions of U-37883A on  $K_{ATP}$  channels in freshly dispersed smooth muscle myocytes using single-channel recordings. Furthermore, it also shows that U-37883A suppressed the peak amplitude of voltage-dependent  $Ba^{2+}$  currents in a concentration- and voltage-dependent manner, at similar concentrations to those inhibiting  $K^+$  channels.

### 4.1. Tissue-selectivity of U-37883A for native $K_{ATP}$ channels

It was reported that U-37883A has no effect on  $K_{ATP}$  currents in the insulinoma-derived RINm5F cells (Guillemare et al., 1994), cardiac myocytes and skeletal muscle cells (Wellman et al., 1999). In contrast, U-37883A inhibited  $K_{ATP}$  currents in arterial smooth muscle, thereby indicating that U-37883A possesses a tissue-selectivity as a vascular  $K_{ATP}$  channel blocker (Wellman et al., 1999). In the present experiments, U-37883A also caused inhibitory effects on macroscopic  $K_{ATP}$  currents recorded with nystatin-perforated patch recording and unitary  $K_{ATP}$  channels in the cell-attached configuration. Furthermore, U-37883A reduced the levcromakalim-induced urethral relaxation. Thus, since it clearly affects non-vascular smooth muscle, it is not appropriate to consider that U-37883A is a selective vascular  $K_{ATP}$  channel blocker.

In the present experiments, some discrepancies remain regarding the potency of U-37883A between macroscopic and unitary  $K_{ATP}$  currents. In the nystatin-perforated patch recording, the basal amplitude of  $K_{ATP}$  current at  $-50$  mV was reduced by extracellular application of 30  $\mu$ M U-37883A to approximately 25% ( $24 \pm 7\%$ ,  $n=4$ ). Whereas, in the cell-attached recording, extracellular application of U-37883A (10–30  $\mu$ M) had little inhibitory effect on the activity of  $K_{ATP}$  channels and a much higher concentration (100  $\mu$ M) was required to reduce their activity. It is probable that the binding site for U-37883A is readily accessible from the extracellular

solution, and that its ability to decrease the activity of  $K_{ATP}$  channels in cell-attached patches when applied extracellularly requires its diffusion through the membrane generating a low concentration for binding site(s). In confirmation is the apparent ability of U-37883A, when included in the pipette solution (100  $\mu$ M) in cell-attached configuration, to prevent extracellular application of levcromakalim (or pinacidil) from activating  $K_{ATP}$  channels. However, we cannot be certain as to the exact binding sites for U-37883A on the  $K_{ATP}$  channels, and further studies may cast light upon the exact nature of the binding and thus identify a potentially useful site for producing more potent blockers for  $K_{ATP}$  channels.

### 4.2. Actions of U-37883A on the channel pore region in $K_{ATP}$ channels

Recent functional expression studies using *Xenopus* oocytes have revealed that U-37883A ( $\leq 100$   $\mu$ M) selectively inhibits  $K_{ATP}$  channels containing Kir6.1 subunits and has no inhibitory effect on the activity of  $K_{ATP}$  channels containing Kir6.2 subunits regardless of the types of co-expressed SURs (SUR1, Surah-Narwal et al., 1999; SUR2B, Kovalev et al., 2001). These results strongly indicate that U-37883A selectively binds to Kir6.1.

In the present experiments, U-37883A had an inhibitory potency on  $K_{ATP}$  currents in nystatin-perforated recordings ( $K_i$ , 4.7  $\mu$ M) similar to its inhibitory potency on  $K_{ATP}$  channels in rat mesenteric artery ( $K_i$ , 3.5  $\mu$ M, Wellman et al., 1999) and recombinant SUR2B/Kir6.1 ( $K_i$ , 3.5  $\mu$ M, Kovalev et al., 2001). Furthermore, in tension measurement, the levcromakalim (1  $\mu$ M)-induced relaxation was also inhibited by U-37883A in pig urethra ( $K_i$ , 0.8  $\mu$ M) with a similar potency to its effects on rat mesenteric artery ( $K_i$ , 1.1  $\mu$ M, Wellman et al., 1999). It is tempting to speculate that the pore forming subunits of pig urethral  $K_{ATP}$  channels are similar to those of vascular  $K_{ATP}$  channels.

However, regarding the effects of U-37883A, there were several discrepancies between pig urethral  $K_{ATP}$  channels and vascular  $K_{ATP}$  channels. Namely, 1) U-37883A did not suppress the levcromakalim-induced urethral relaxation to the control level, there remaining a U-37883A-insensitive component. 2) U-37883A (100–300  $\mu$ M) did not abolish the levcromakalim-induced  $K_{ATP}$  currents and the remaining small but significant U-37883A-insensitive  $K_{ATP}$  currents were readily abolished by glibenclamide. 3) In cell-attached mode, activity of  $K_{ATP}$  channels was still observed even in the presence of 100  $\mu$ M U-37883A although the activity of  $K_{ATP}$  channels was suppressed by 10  $\mu$ M glibenclamide. These results suggest that the nature of the channel pore regions in pig urethral  $K_{ATP}$  channels assessed by the effects of U-37883A is not identical to that of vascular  $K_{ATP}$  channels.

### 4.3. Inhibitory effects of U-37883A on the voltage-dependent $Ba^{2+}$ currents in pig urethra

The same amplitude of voltage-dependent  $Ba^{2+}$  currents was produced when holding at  $-80$  mV or more negatively,



suggesting that all of the voltage-dependent  $\text{Ca}^{2+}$  channels at these potentials may be in the resting state. The ability of 10  $\mu\text{M}$  U-37883A to suppress the peak amplitude of the  $\text{Ba}^{2+}$  currents evoked by a depolarizing pulse from two different holding potentials ( $-90$  and  $-120$  mV) was not significantly different, suggesting that at these negative holding potentials U-37883A may inhibit the voltage-dependent  $\text{Ba}^{2+}$  currents in a voltage-independent manner (resting state block).

When the holding potential was elevated to  $-50$  from  $-90$  mV, voltage-dependent inhibition by U-37883A was observed and the concentration response curve was shifted to the left. The voltage-dependent inactivation curve was also shifted to the left after application of 30  $\mu\text{M}$  U-37883A. These results suggest that the voltage-dependent inhibitory action of U-37883A occurs at the inactivated state of voltage-dependent  $\text{Ca}^{2+}$  channels in pig urethra (voltage-dependent block).

In the present experiments, the  $K_{\text{rest}}$  value was estimated to be 46  $\mu\text{M}$  from the concentration response curve at a holding potential of  $-90$  mV. When  $\Delta V_{\text{half}}$  value was obtained from the results using 8 s conditioning pulses, the estimated  $K_{\text{inact}}$  value was 9  $\mu\text{M}$ . Given this, we suggest that U-37883A may bind to the inactivated state with approximately 5 times higher affinity than to the resting state in pig urethra.

#### 4.4. Multiple effects of U-37883A on the membrane currents

Recently, using Kir6.1/Kir6.2 chimera studies, Kovalev et al. (2004) have reported that the C-terminus of Kir6.1 is an important determinant of the ability of U-37883A to inhibit channel activity even when constructs were co-expressed with SUR1 or SUR2B. Since structural differences between Kir6.1 and Kir6.2 are important in determining sensitivity to U-37883A, Kovalev et al. (2004) suggest that U-37883A may prove useful in probing the structural and functional differences between Kir6.1 and Kir6.2 subtypes. However, U-37883A can inhibit several types of  $\text{K}^{+}$  channels in a wide variety of cells (see Introduction), including  $\text{BK}_{\text{Ca}}$  channels in pig urethra (Teramoto et al., 2004). Furthermore, in the present experiments, we have demonstrated that U-37883 had inhibitory effects on  $\text{K}_{\text{ATP}}$  channels and voltage-dependent  $\text{Ba}^{2+}$  currents at a similar concentration range. Thus, in smooth muscle, U-37883A may be considered not only a blocker of multiple  $\text{K}^{+}$  channels but also a voltage-dependent  $\text{Ca}^{2+}$  channel blocker.

#### 4.5. The presence of relaxing mechanisms different from those of the glibenclamide-sensitive effects in pig urethra

Pig urethral smooth muscles relax in response to nitric oxide (NO) release from nitrergic nerves (Bridgewater et al., 1993). As SNP is thought to be a potent exogenous NO generator, it is reasonable to assume that SNP-induced relaxation may utilize the same mechanisms. In the present experiments, the SNP-induced urethral relaxation attained a similar sustained level to that obtained with levromakalim, even at the same concentration, although this was achieved more quickly, and, more importantly, was insensitive to subsequent application of

glibenclamide (1–10  $\mu\text{M}$ ). These results suggest that the SNP-induced urethral relaxation occurs through a mechanism other than opening of  $\text{K}_{\text{ATP}}$  channels, but that there may be a maximum level of relaxation attainable by either route.

In conclusion, U-37883A inhibited  $\text{K}_{\text{ATP}}$  channels and voltage-dependent  $\text{Ca}^{2+}$  channels in pig urethra. Therefore, it is not feasible to define U-37883A as a vascular  $\text{K}_{\text{ATP}}$  channel blocker since U-37883A possesses neither tissue selectivity nor ion channel selectivity.

#### Acknowledgments

We thank Dr. N.J. Bramich (University of Melbourne, Department of Zoology, Melbourne, Australia) for critical reading of the manuscript. This work was supported by both a Grant-in-Aid for Scientific Research (B)-(2) from the Japanese Society for the Promotion of Science (Noriyoshi Teramoto, Grant Number 16390067) and a Grant-in-Aid for Exploratory Research from the Ministry of Education and Culture of Japan (Noriyoshi Teramoto, Grant Number 17659075). This work was also supported in part by a grant-in-aid from the Japanese Society for the Promotion of Science to young research fellowship (Takakazu Yunoki, Grant Number 14PD-08992).

#### References

- Aguilar-Bryan, L., Nichols, C.G., Wechsler, S.W., Clement IV, J.P., Boyd, A.E., González, G., Herrera-Sosa, H., Nguy, K., Bryan, J., Nelson, D.A., 1995. Cloning of the  $\beta$  cell high-affinity sulfonylurea receptor: a regulator of insulin secretion. *Science* 268, 423–425.
- Babenko, A.P., Aguilar-Bryan, L., Bryan, J., 1998. A view of SUR/KIR6.x,  $\text{K}_{\text{ATP}}$  channels. *Annu. Rev. Physiol.* 60, 667–687.
- Bridgewater, M., MacNeil, H.F., Brading, A.F., 1993. Regulation of tone in pig urethral smooth muscle. *J. Urol.* 150, 223–228.
- Guillemare, E., Honore, E., De Weille, J., Fosset, M., Lazdunski, M., Meisheri, K., 1994. Functional receptors in *Xenopus* oocytes for U-37883A, a novel ATP-sensitive  $\text{K}^{+}$  channel blocker: comparison with rat insulinoma cells. *Mol. Pharmacol.* 46, 139–145.
- Inagaki, N., Gono, T., Clement IV, J.P., Namba, N., Inazawa, J., González, G., Aguilar-Bryan, L., Seino, S., Bryan, J., 1995. Reconstitution of IKATP: an inward rectifier subunit plus the sulfonylurea receptor. *Science* 270, 1166–1170.
- Kovalev, H., Lodwick, D., Quayle, J.M., 2001. Inhibition of clone  $\text{K}_{\text{ATP}}$  channels by the morpholinoguanidine PNU-37883A. *J. Physiol.* 531P, 89P–90P.
- Kovalev, H., Quayle, J.M., Kamishima, T., Lodwick, D., 2004. Molecular analysis of the subtype-selective inhibition of cloned  $\text{K}_{\text{ATP}}$  channels by PNU-37883A. *Br. J. Pharmacol.* 141, 867–873.
- Lin, Y.J., Chen, X., Freedman, J.E., 1998. U-37883A potently inhibits dopamine-modulated  $\text{K}^{+}$  channels on rat striatal neurons. *Eur. J. Pharmacol.* 352, 335–341.
- Meisheri, K.D., Humphrey, S.J., Khan, S.A., Cipkus-Dubray, L.A., Smith, M.P., Jones, A.W., 1993. 4-morpholinecarboximidine-*N*-1-adamantyl-*N'*-cyclohexylhydrochloride (U-37883A): pharmacological characterization of a novel antagonist of vascular ATP-sensitive  $\text{K}^{+}$  channel openers. *J. Pharmacol. Exp. Ther.* 266, 655–665.
- Surah-Narwal, S., Xu, S.Z., McHugh, D., McDonald, R.L., Hough, E., Cheong, A., Partridge, C., Sivaprasadarao, A., Beech, D.J., 1999. Block of human aorta Kir6.1 by the vascular  $\text{K}_{\text{ATP}}$  channel inhibitor U37883A. *Br. J. Pharmacol.* 128, 667–672.
- Teramoto, N., Aishima, M., Zhu, H.L., Tomoda, T., Yunoki, T., Takahashi-Yanaga, F., Brading, A.F., Ito, Y., 2004. Effects of U-37883A on intracellular  $\text{Ca}^{2+}$ -activated large conductance  $\text{K}^{+}$  channels in pig proximal urethral myocytes. *Eur. J. Pharmacol.* 506, 1–7.

- Teramoto, N., Brading, A.F., 1996. Activation by levromakalim and metabolic inhibition of glibenclamide-sensitive K channels in smooth muscle cells of pig proximal urethra. *Br. J. Pharmacol.* 118, 635–642.
- Teramoto, N., Ito, Y., 1999. Comparative studies on the relaxing action of several adenosine 5'-triphosphate-sensitive K<sup>+</sup> channel openers in pig urethra. *J. Smooth Muscle Res.* 35, 11–22.
- Teramoto, N., Brading, A.F., Ito, Y., 2003. Multiple effects of mefenamic acid on K<sup>+</sup> currents in smooth muscle cells from pig urethra. *Br. J. Pharmacol.* 140, 1341–1350.
- Uehara, A., Hume, J.R., 1985. Interactions of organic calcium channel antagonists with calcium channels in single frog atrial cells. *J. Gen. Physiol.* 85, 621–647.
- Wang, T., Wang, W.H., Klein-Robbenhaar, G., Giebisch, G., 1995. Effects of a novel K<sub>ATP</sub> channel blocker on renal tubule function and K channel activity. *J. Pharmacol. Exp. Ther.* 273, 1382–1389.
- Wellman, G.C., Barrett-Jolley, R., Koppel, H., Everitt, D., Quayle, J.M., 1999. Inhibition of vascular K<sub>ATP</sub> channels by U-37883A: a comparison with cardiac and skeletal muscle. *Br. J. Pharmacol.* 128, 909–916.